Λdoublet substate specific investigation of rotational and fine structure transitions in collisions of OH with H2 and D2

P. Andresen, N. Aristov, V. Beushausen, D. Häusler, and H. W. Lülf

Citation: The Journal of Chemical Physics **95**, 5763 (1991); doi: 10.1063/1.461598
View online: http://dx.doi.org/10.1063/1.461598
View Table of Contents: http://scitation.aip.org/content/aip/journal/jcp/95/8?ver=pdfcov
Published by the AIP Publishing

Λ-doublet substate specific investigation of rotational and fine structure transitions in collisions of OH with H_2 and D_2

P. Andresen, N. Aristov, V. Beushausen, D. Häusler, and H. W. Lülf
Max-Planck-Institut für Strömungsforschung, 34 Göttingen, Germany

(Received 28 August 1989; accepted 10 July 1991)

The selective population of rotational, spin, and Λ-doublet states of OH($^2\Pi, v = 0,1$) by inelastic collisions with H_2 and D_2 is investigated in two experiments. In the first experiment OH radicals are generated by photolysis inside a pulsed nozzle beam source and prepared in the ground state $j = 1.5$, $v = 0$, $^2\Pi_{3/2}$ with equal amounts in both Λ-doublets by rotational cooling in the subsequent expansion. The collisional excitation of OH by the secondary beam is probed via laser-induced fluorescence selectively for the Λ-doublet states for the different rotational levels in both spin manifolds of $v = 0$. Integral cross sections $\sigma(j = 1.5, \bar{\Omega} = 1.5 \rightarrow j', \bar{\Omega}', \epsilon')$ averaged over the Λ-doublet substates in the input channel, but Λ-doublet substate resolved in the output channel are obtained in this case. In contrast to some previous predictions the $\Pi(A')$ Λ-doublet substate is preferentially populated. This implies a population inversion in the Λ-doublets for $^2\Pi_{1/2}$ and an anti-inversion for $^2\Pi_{3/2}$, which rules out previously proposed pump mechanisms for astronomical OH masers. In the second experiment OH is generated also by photolysis, in this case however in a flow system. Single Λ-doublet states are prepared by infrared excitation of the thermally relaxed OH in $^2\Pi_{3/2}$, $v = 1$ for two rotational states ($j = 1.5, 4.5$). The redistribution in $v = 1$ induced by collisions with H_2 is probed by laser-induced fluorescence. Rate constants are obtained for transitions from the initially prepared Λ-doublet states to the other Λ-doublet of the same j and also for transitions to other rotational states.

I. INTRODUCTION

More than 20 years ago an intense microwave emission resulting from different Λ-doublet transitions in OH was observed from the interstellar medium. The high brightness temperature of this emission could only be explained by natural maser activity.[1] The origin of the population inversion between the Λ-doublet states remained however unclear and was the subject of many investigations since then. Some years ago the most probable explanation for masers the $^2\Pi_{3/2}$ multiplet states still seemed to be collisional excitation of OH by species such as H, H_2, or electrons.[2–5]

Recent experiments have shown that several processes, as OH-producing chemical reactions[6] or photodissociation of H_2O,[7] H_2O_2,[8] and HNO_3[9] do indeed yield OH preferentially in Λ-doublet states, i.e., they favor the production of one Λ-doublet substate over the other. This behavior was qualitatively understood in terms of conservation of electronic reflection symmetry in planar dissociation events going from parents to products. At least in the high j limit the Λ-doublet states are either symmetric [$\Pi(A')$] or antisymmetric [$\Pi(A'')$] with respect to the plane of rotation.[10] [Note that we use here the recently devised nomenclature for Λ-doublet substates,[11] i.e., $\Pi(A')$ and $\Pi(A'')$, which shows directly the symmetry of the wave functions with respect to the plane of rotation.] The formation of OH in the $\Pi(A')$ or $\Pi(A'')$ is then expected along A' or A'' potential surfaces, respectively. The analysis of the above mentioned experiments[6,7,7(a),9] suggests another association between symmetry and energetical ordering of the Λ-doublet substates than used in the above mentioned attempts to explain the pump mechanism of OH masers. Meanwhile, the confusion about the assignment of symmetry versus energetical ordering of the Λ-doublets—originating from the theoretical studies about the OH–H_2 pump mechanism predicting inversion between the Λ-doublets in the $^2\Pi_{3/2}$—has been clarified in favor of the experimental evidence. For more details the reader is referred to the careful analysis by Alexander and Dagdigian,[10] which agrees with Refs. 6, 7, and 9, but contradicts Refs. 2, 4, and 5(a).

Nevertheless there were no direct experiments to prove whether inelastic collisions of OH with hydrogen yields inversion or anti-inversion between the Λ-doublets in either $^2\Pi_{3/2}$ or $^2\Pi_{1/2}$. This study proves that collisional excitation of OH leads to inversion in $^2\Pi_{1/2}$ and anti-inversion in $^2\Pi_{3/2}$. The present paper extends on the results of a previous publication[12] and deals with two complementary experiments. In the first experiment integral cross sections are measured in a crossed beam experiment for the processes

$$\mathrm{OH}(v = 0, j = 1.5, \bar{\Omega} = 1.5, \epsilon = \pm 1) + \mathrm{H_2}\,(\mathrm{D_2}) \rightarrow \mathrm{OH}(v = 0, j', \bar{\Omega}', \epsilon') + \mathrm{H_2}\,(\mathrm{D_2}). \quad (1)$$

Here j is the total angular momentum and $\bar{\Omega} = |\Lambda + \Sigma|$, where Λ and Σ are the projections of the electronic and spin angular momentum onto the internuclear axis. The value of ϵ is related to the parity of the OH electronic wave function and as such an index for the Λ-doublet sublevels.

Both multiplet conserving and multiplet changing transitions are investigated. The OH molecules in $v = 0$ are produced by photodissociation of HNO_3. The beam consists almost exclusively of molecules in the $j = 1.5$ level of the

 0021-9606/91/205763-12$03.00

$^2\Pi_{3/2}$ state with equal population in the Λ-doublets. The population in a specific Λ-doublet, j' and $\bar{\Omega}'$ level of OH is probed by laser-induced fluorescence (LIF). The experiment shows inversion between Λ-doublets in $^2\Pi_{1/2}$ and antiinversion in $^2\Pi_{3/2}$, a result that is in direct contradiction to the collisional pump mechanism proposed for astronomical OH masers. Because both Λ-doublets are populated in the primary beam, the cross sections are averaged over initial Λ-doublet states but specific in the product channel.

A better state preparation is achieved in a second experiment, in which the reactant OH is produced in a unique Λ-doublet sublevel by infrared excitation to $v=1$. Comparable experiments with preparation of single initial Λ-doublet states have been performed in excited Π states,[13] where the preparation is simply achieved by using appropriate excitation frequencies. Preparation of a single quantum states in the electronic ground state is much harder. The method adopted here is selective infrared excitation.[14] The OH radicals are first generated by photolyzing a mixture of H_2O_2 and H_2 in a flow system. After a certain delay (to equilibrate OH to room temperature) the OH is vibrationally excited with a pulsed infrared laser. The preparation of single Λ-doublets of one specific rotational state in $v=1$ is possible because of the selection rules for infrared (IR) absorption. The subsequent collision induced change in the population of $OH(v=1)$ states is probed as function of time by LIF.

The collisional processes

$$\mathrm{OH}(v=1,j=1.5,4.5,\bar{\Omega}=1.5,\epsilon=+1,-1)+\mathrm{H_2} \rightarrow \mathrm{OH}(v'=1,j'=1.5,4.5,\bar{\Omega}'=1.5,\epsilon'=-1,+1)+\mathrm{H_2}, \quad (2)$$

$$\mathrm{OH}(v=1,j=1.5,4.5,\bar{\Omega}=1.5,\epsilon=+1,-1)+\mathrm{H_2} \rightarrow \mathrm{OH}(v'j',\bar{\Omega}',\epsilon')+\mathrm{H_2}, \quad \text{with } j\neq j' \text{ if } \bar{\Omega}=\bar{\Omega}' \text{ and } v=v', \quad (3)$$

are studied. Fitting the experimental data by using rate equations we obtain the state to state rate constants k_Λ for the energy transfer between the Λ-doublet substates of the prepared rotational level (process 2) and the "total" rate constants $k_R(A')$ and $k_R(A'')$ for transitions from the $\Pi(A')$ and $\Pi(A'')$ Λ-doublet substates, respectively, of the prepared rotational level to all final states (processes 3).

In the calculations it turned out that the use of a coupling potential that depends on the azimuthal angle Φ[15] can lead to a phase error.[16,17] This error is avoided using an alternative description of the coupling mechanism proposed by Alexander,[18] which does not use a Φ dependent potential. The publication of our earlier results[11] suggested a new theoretical investigation of the OH–H_2 scattering.[19–21] Because the earlier errors are avoided, reasonably good agreement between theory and experiment could be achieved. Remaining discrepancies are suspected to be due to shortcomings in the *ab initio* potential surface.[19] Recently, also hyperfine transitions have been studied.[22] The preferential population of the $\Pi(A')$ Λ-doublet level has been interpreted in terms of the π^3 electron occupancy of OH.[23] In this work the influence of the shape of the difference potential on the population of the Λ-doublet states is studied in some detail.

II. EXPERIMENTAL

A. Crossed beam experiment

1. General

Figure 1 shows the setup for the crossed beam experiment. The OH and H_2 (D_2) beams are produced in pulsed modified fuel injection valves and cross each other at 90°. The stagnation pressure in the H_2 source is 100 Torr. The OH radicals are generated by photodissociation of HNO_3 in a quartz capillary (1 mm inner diameter, 10 mm long) mounted in front of the nozzle orifice. Because the radicals are produced inside the stagnation region possible broadening of the angular and velocity distribution are avoided.[24,25] For optimum rotational cooling of the OH the HNO_3 is seeded in argon with a typical HNO_3/Ar ratio of 1:10 using stagnation pressures ~200 Torr. HNO_3 is chosen as a precursor because of its large absorption coefficient [1.2×10^{-17} cm^2 (Ref. 26)] at 193 nm. The ArF photolysis laser (Lambda Physik EMG 200) has a pulse length of 12 ns and an energy of 200 mJ/pulse. The laser beam is slightly focused to the capillary using a 1 m lens. Further details on the OH beam are given below.

Both the OH and H_2 beams are collimated by skimmers ~10 mm downstream the nozzles. The interaction region is located 30 mm away from the nozzles. The OH state distributions are probed via the OH $A\,^2\Sigma \rightarrow X\,^2\Pi$ absorption band with a frequency doubled Nd-YAG pumped dye laser operating ~310 nm. Its frequency doubled output is ~3 mJ with a linewidth of ≃0.45 cm^{-1}. This is sufficient to saturate most of the measured transitions and to resolve the rotational spectrum. The probe laser passes through a system of apertures to cut off the wings.

The probe laser irradiates the scattering center perpendicularly to both beams. The OH fluorescence is collected from a small area by an imaging optics mounted in the scattering plane at an angle of 45° relative to the molecular beams with an EMI 9813QB phototube. A Schott color filter (UG11) and a cone in front of the imaging optics suppresses daylight and scattered laser light, respectively. Light baffles are placed along the path of the probe laser beam to further reduce laser scatter. The resulting signal is averaged in a boxcar integrator and displayed on a chart recorder. The gate of the boxcar is set to collect all fluorescence. In parallel the laser power is monitored by a photodiode.

As mentioned above, the interaction region is located very close to the nozzles, i.e., 30 mm away. The resulting high particle densities yield good signal to noise ratios. The measuring time to record one cross section is typically 15 min. However, it does require careful timing of the pulsed valves versus the dissociation laser, so that single collision conditions are maintained throughout the probing time. The photolysis laser is fired after the HNO_3 beam has reached steady state conditions in the capillary to achieve good cooling of the OH radicals.[27] On the other hand the laser should be as close as possible to beginning of the pulse to avoid backscatteringin the interaction region. The optimum delay time between the beginning of the HNO_3 pulse and the firing of the dissociation laser is thus found to be between 200 and 300 μs. The best time for the probe laser is found by simply

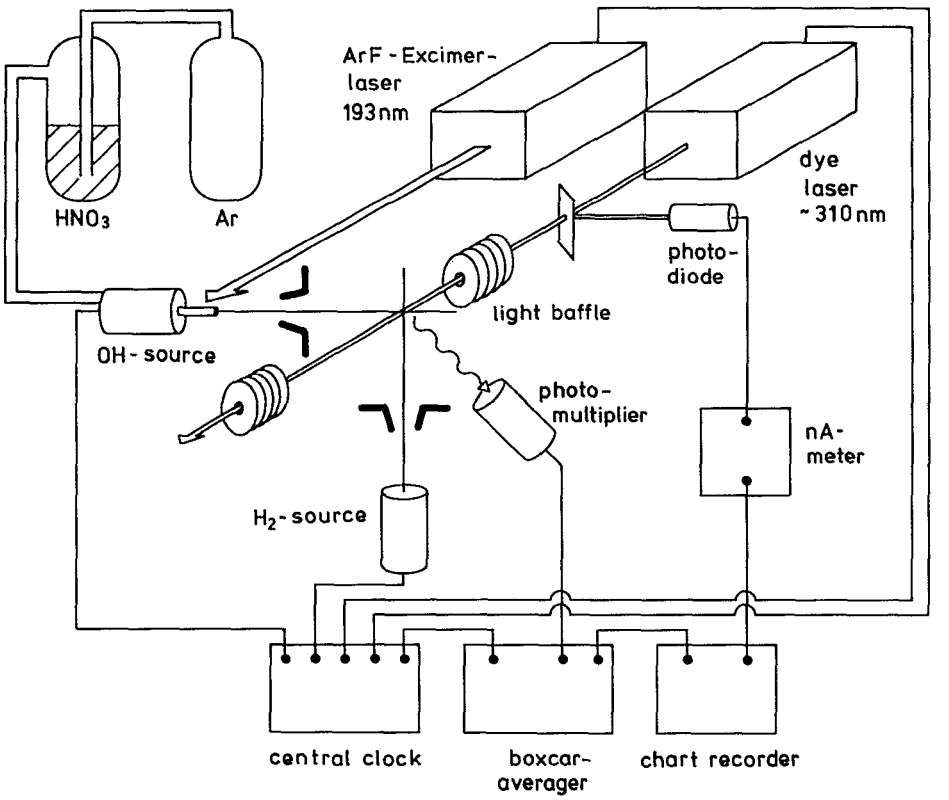

FIG. 1. Crossed beam apparatus.

scanning its delay time with respect to the photolysis laser until a maximum OH signal is obtained. Single collision conditions are carefully tested by inspecting the spectrum at a series of decreasing stagnation pressures until the relative line intensities stay the same. The procedure was done for all source pressures used.

2. Reactant and product characterization

Figure 2 shows the time profile of the OH pulse. It is measured by tuning the probe laser to the peak of an OH transition and then sweeping the delay time between the two lasers. The overall length of the pulse is 40 μs and is determined by the mean beam velocity, the velocity distribution, and the length of the quartz tube. Note that only those HNO_3 molecules are dissociated, which are in the capillary tube, when the ArF laser is fired. The pulse is asymmetric, with a fast onset and a slow decay. The peak density lasts only a few microseconds. The decay is attributed to fast secondary reactions in the quartz tube: the further upstream the OH radicals are produced, the longer they reside in the capillary and the higher is the probability for recombination reactions. A crude estimate[28] for the intensity of the OH beam yields $\sim 10^{19}$ molecules/sr s, corresponding to an OH density in the scattering center of $\simeq 10^{13}$ molecules/cm^3. The estimate is based on the assumption that the HNO_3 is completely dissociated (which is reasonable considering the large absorption coefficient), and that a capillary instead of an "ideal" nozzle hole leads to a reduction of the particle flux by a factor of 2.[29]

The state distribution in the primary OH beam is measured in the scattering center with the secondary beam off. Figure 3 shows the corresponding results in a Boltzmann plot. The beam consists obviously almost exclusively of ground state OH molecules in the state $^2\Pi_{3/2}, j = 1.5$ with equal population in both Λ-doublet states. The population in this state is at least 10 times larger than in any other state. Roughly 23% of the molecules are in excited states. As can be seen, the plot deviates from a straight line indicating that the molecules are not in thermal equilibrium. This non-Boltzmann behavior has been observed in several other cases[30,31] and is due to "freezing" of the higher levels. To qualitatively characterize the beam by some temperature, a

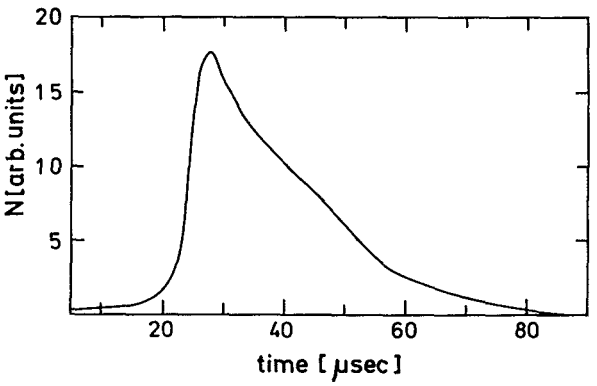

FIG. 2. Time profile of the ground state $j = 1.5$, $^2\Pi_{3/2}$ of the reactand OH.

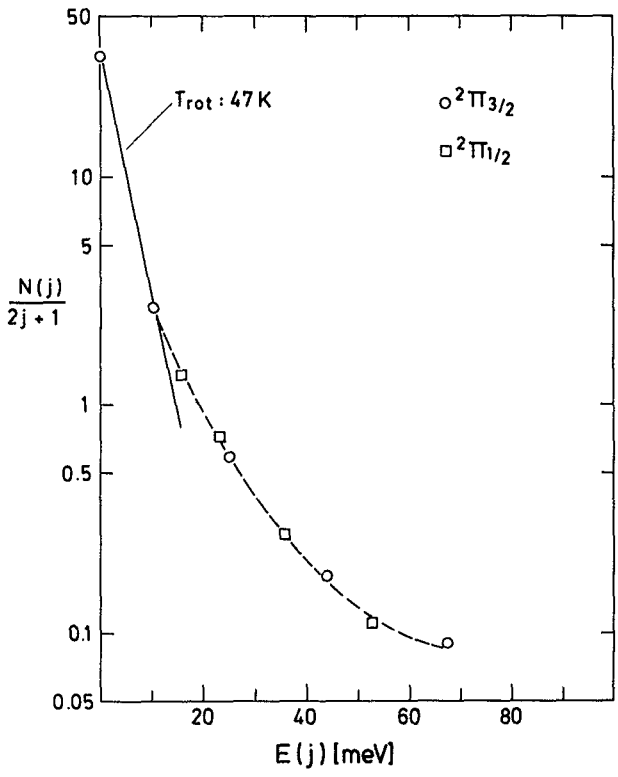

FIG. 3. State distribution in the $^2\Pi_{3/2}$ manifold (○) and the $^2\Pi_{1/2}$ manifold (□) of the OH reactand beam.

straight line is drawn through the lowest two rotational states. This line corresponds to a rotational "temperature" of ~50 K. The rotational cooling is obviously very efficient, considering that the OH is formed in the quartz capillary with an initial temperature of ~2000 K.[9]

The existence of ortho and para modifications in normal H_2 and D_2 leads to a dominant population of $j=1$ in the H_2 and $j=0$ in the D_2 beam. According to the statistical weights in the H_2 beam only 25% of the molecules are in $j=0$ and 75% in $j=1$, whereas for D_2 67% of the molecules are in $j=0$ and 33% in $j=1$.

The collision energies are calculated under the reasonable assumption of a complete expansion. This yields 83 meV for the OH–H_2 system and 78 meV for OH–D_2. At these energies the following product OH channels can be excited: $j'=1.5$–5.5 in $^2\Pi_{3/2}$, $v=0$ and $j'=0.5$–4.5 in $^2\Pi_{1/2}$, $v=0$.

The two OH Λ-doublet states are probed via different branches of the $^2\Sigma$–$^2\Pi$ band:[32] $\Pi(A')$ levels are probed via the lines $R_1(2)$–$R_1(5)$ and $R_2(1)$–$R_2(4)$, $P_2(5)$; and $\Pi(A'')$ levels are probed via $Q_1(2)$, $S_1(3)$, $Q_1(4)$, $Q_1(5)$ and $Q_2(1)$, $O_2(3)$–$O_2(5)$. It will be emphasized that each spectral line can be unambiguously related to a particular Λ-doublet substrate. Thus, the energy ordering of the doublet, i.e., whether it is the lower or upper level, is known.

3. Derivation of cross sections

The OH radicals are probed with a pulsed laser and the lifetime of the excited $^2\Sigma$ state is short compared to the residence time of the molecules in the field of view of the detector. Thus, with the *particle density* n_i in the probed state we obtain,[33]

$$I(i) = n_i \cdot F(i,f), \tag{4}$$

where I is the fluorescence signal and the indices i and f denote the initial and final state of the excitation process. The factor F contains the excitation probability, the detection efficiency for fluorescence and the volume of the interaction region of laser and molecular beam.[33] The detection probability and the geometry of laser and molecular beam are independent of i and f for all probed rotational levels.

In the R_1, P_2, and Q branches the main lines are neighbored by weak satellite lines.[32] However for most of the probed levels satellite and main lines are sufficiently apart to ensure an exclusive excitation of the main line. The energy of the probe laser is sufficiently high to saturate transitions in the main branches, i.e., Q, P, and R lines. The wings of the laser beam, where the energy may be below the value necessary for saturation, are cut off by an aperture. Saturation in a two level system implies that the excitation probability is 50% independent of the probed level and the laser power. In this case we obtain for the density of OH molecules scattered into a quantum state i,

$$n_i^s \sim I_{on}(i) - I_{off}(i), \tag{5}$$

where I_{on} and I_{off} are the fluorescence signals obtained with the H_2 (D_2) beam on and off.

For the $Q_2(1)$ line the satellite line is very close, i.e., 0.25 cm^{-1}, so that it is also excited by the probe laser. Hence the excitation rate is > 50% and the fluorescence signal cannot be compared directly to the signals obtained via the other lines.

For P lines not all the m_j sublevels of the ground state are coupled to the excited state. Δj is minus one here and only transitions with $\Delta m_j = 0$ are allowed. Thus the excitation rate is lower than 50% and it depends on the rotational level. In the experiment only the level with $j'=4.5$, $\overline{\Omega}=0.5$ is probed via a P line. The measured n_i^s is normalized to the values obtained via R lines by multiplying it with a factor of 1.25.

In principle, for the evaluation of cross sections each n_i^s has to be transformed into a flux of particles.[34] However, OH is heavy compared to H_2 or D_2 which implies that the motion of the scattered OH (in the laboratory system) is dominated by the center of mass velocity. In this case the influence of the density to flux transformation is small so that the use of the measured densities introduce minor errors in the integral cross sections.

Since $j=1.5$, $\overline{\Omega}=1.5$ is prepared, we obtain

$$\sum_{\epsilon} \sigma(j=1.5,\overline{\Omega}=1.5,\epsilon \rightarrow i) \sim I_{on}(i) - I_{off}(i). \tag{6}$$

Note that the *sum* of the two cross sections for $\epsilon = +1$ and $\epsilon = -1$ is measured, because the Λ-doublet substates of the rotational ground state are equally probable in the primary beam. For this sum the following notation will be introduced:

$$\sum_{\epsilon} \sigma(j=1.5,\bar{\Omega}=1.5,\epsilon \rightarrow j',\bar{\Omega}',\epsilon') = \sigma_{A'}(j',\bar{\Omega}')$$

if ϵ' denotes a $\Pi(A')$ level $= \sigma_{A''}(j',\bar{\Omega}')$

if ϵ' denotes a $\Pi(A'')$ level. (7)

The relative population between the Λ-doublets is consequently $\sigma_{A'}/\sigma_{A''}$.

All $\Pi(A')$ levels are probed via saturated R and P lines. Thus the cross sections $\sigma_{A'}(j',\Omega')$ can be determined with Eq. (6). However many of the $\Pi(A'')$ levels are probed via transitions with an excitation efficiency other than 50%: S and O lines are not completely saturated. Here the excitation rate becomes a function of the Hönl–London factors and depends on rotational state as well as on the energy of the probe laser.[33] Also the $Q_2(1)$ line is overlapped by a satellite line. These problems are solved by using the fact that there is an equal population of the Λ-doublet substates in the primary beam. With Eqs. (4) and (6) the ratio $\sigma_{A'}/\sigma_{A''}$ for a specific $j',\bar{\Omega}'$ is obtained as

$$\frac{\sigma_{A'}}{\sigma_{A''}} \sim \frac{[I_{on}(A') - I_{off}(A')]\cdot F(A'')}{[I_{on}(A'') - I_{off}(A'')]\cdot F(A')}. \quad (8)$$

From Eq. (4) it follows that with the H_2 beam off the ratio of the LIF signals obtained for the two Λ-doublet substates of a specific $j',\bar{\Omega}'$ is inversely proportional to the corresponding factors $F(A')$ and $F(A'')$, since in the primary beam the Λ-doublet substates are equally populated, i.e., $n_i(A') = n_i(A'')$.

With Eq. (8) we obtain

$$\frac{\sigma_{A'}}{\sigma_{A''}} = \frac{[I_{on}(A') - I_{off}(A')]\cdot I_{off}(A'')}{[I_{on}(A'') - I_{off}(A'')]\cdot I_{off}(A')}. \quad (9)$$

Equation (9) shows that the ratio $\sigma_{A'}/\sigma_{A''}$ is only a function of fluorescence intensities. The effect of the excitation rate is cancelled out. Now the values of the $\sigma_{A''}$ can be easily normalized to the values of the cross sections $\sigma_{A'}$ by first determining $\sigma_{A'}$ and $\sigma_{A'}/\sigma_{A''}$ from the experimental data and then calculating $\sigma_{A''}$ via

$$\sigma_{A''} = \frac{\sigma_{A'}}{(\sigma_{A'}/\sigma_{A''})}. \quad (10)$$

B. Double resonance experiment

1. General

The setup of the double resonance experiment shown in Fig. 4 is similar to that used in an earlier experiment.[35] The central part is a flow system consisting of a stainless steel tank with a 100 mm inner diameter. It is evacuated by a roughing pump via an adjustable valve to regulate the output flow. The pressure is measured with an MKS Baratron. Needle valves in the feed pipes of H_2 and H_2O_2 are used to control the input flow. The partial pressures of H_2 and H_2O_2 (250 and 50 mTorr, respectively) are adjusted by first feeding the flow system with H_2 until a pressure of 250 mTorr is obtained and then adding H_2O_2 until an overall pressure of 300 mTorr is reached. This gas mixture is chosen to obtain a reasonably high concentration of OH and nevertheless have the OH collisions dominated by H_2 and not by its precursor H_2O_2. The overall pressure is low to be close to

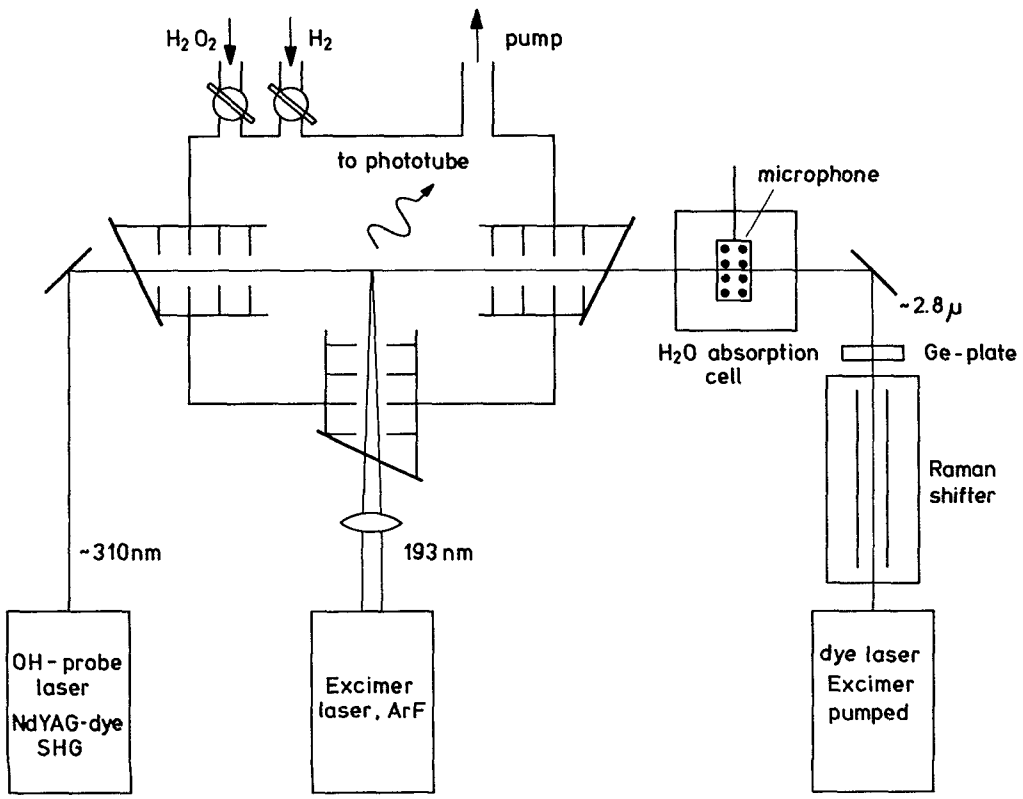

FIG. 4. Double resonance apparatus.

single collision conditions in $v = 1$ after IR excitation. The purity of the H_2O_2 is 98%. All measurements are performed at 300 K.

The pulsed laser systems and the detection electronics used in the crossed beam experiment are also used here. The ArF-laser is used to dissociate the H_2O_2 and the tunable ultraviolet (UV)-laser to probe the vibrationally excited OH. The OH fluorescence is detected perpendicularly to the laser beams. The preparation of the quantum states in $OH(v = 1)$ is achieved with an additional third laser system, an excimer-pumped dye laser (Lambda Physik EMG200, F2002E), whose linewidth is reduced to 0.04 cm^{-1} by an intracavity étalon, and which has an output energy of $\simeq 50$ mJ/pulse. The 610 nm light is focused into a Raman shifter filled with 25 bar H_2. To improve the Raman efficiency, a waveguide is mounted in the cell.[36] By filtering out the third Stokes line with a coated germanium plate, tunable infrared light near 2.8 μm, with an output energy of 0.5 mJ/pulse and the same linewidth as the dye laser, i.e., 0.04 cm^{-1} is obtained. To avoid photon losses due to absorption by water vapor, the beam path of the infrared light is flushed with dry N_2.

The wavelength of the IR laser is determined by an infrared absorption spectrum of water[37] using the photoacoustic technique:[35,38] the laser beam passes through a small cell filled with 18 Torr H_2O, in which a microphone is mounted close to the beam path. Whenever the laser is tuned to an H_2O absorption wavelength, a sound wave is generated and registered by the microphone. The H_2O spectrum is easily identified and used to determine the precise wavelength of the tunable IR. In order to find and excite a given OH level[39] the laser is scanned only over the range of the two nearest H_2O lines.

The infrared and probe laser beam are antiparallel and perpendicular to the beam of the dissociation laser, which is focused to the crossing point. All three beams enter the flow chamber (and the photoacoustic cell) through CaF_2 windows set at Brewster angles to reduce stray light. A central clock is used to trigger the lasers and the boxcar integrator.

2. Reactant characterization

First experiments with HNO_3 as precursor for OH were not successful for two reasons. First, an intense long lasting emission, presumably due to fluorescence of electronically excited NO_2, disturbed the measurements. Second, OH was produced to a considerable extent in $v = 1$, destroying the state preparation by IR excitation. Therefore H_2O_2 was used as precursor, although the absorption cross section is $\sim 10\times$ smaller than for HNO_3, i.e., $\simeq 6.5\times 10^{-19}$ cm^2.[40] In this case almost no vibrationally excited OH is formed and the background emission is highly reduced.

The photodissociation of H_2O_2 has been studied by several authors.[8,9] The OH is formed essentially in the ground electronic and vibrational states, with $<5\%$ in $v = 1$. The spin states were found to be equally populated, whereas one Λ-doublet turns out to be slightly favored [$\Pi(A')$]. The distribution of rotational states is rather broad with a maximum at $j = 6.5$.

The IR laser is fired several microseconds after the dissociation laser pulse. This is done to obtain thermalized OH at 300 K. The $\Pi(A')$ and $\Pi(A'')$ Λ-doublet substates of rotational levels with $j = 1.5, 4.5$ in $v = 1$, $^2\Pi_{3/2}$ are prepared by IR excitation. The $OH(v = 1)$ population from photolysis is negligible for the experiment: with IR excitation the LIF signal out of the prepared state in $v = 1$ increases by at least a factor of 50.

Based on Beer's law it is estimated that $\sim 10\%$ of the H_2O_2 molecules are dissociated. The number of OH radicals that are subsequently excited by the IR laser to the desired initial quantum level can be estimated using the tabulated Einstein coefficients[41] after accounting for the distribution of the rotational levels in $v = 0$. Under the given experimental conditions, we estimate that the ratio of prepared OH in the $j = 1.5(4.5)$, $v = 1$ level to the reactant H_2O_2 is only 0.01 (0.006).

3. Rate constant determination

The collisional redistribution is probed via the $Q_1(1)$ and $R_1(1)$ line (prepared $j = 1.5$) and the $Q_1(4)$ and $R_1(4)$ line (prepared $j = 4.5$) of the 1–1 band of the OH $^2\Sigma \rightarrow {}^2\Pi$ transition.[32(a)] The LIF signals are proportional to particle densities (see Sec. II A 3). Measured are the populations in the Λ-doublet substates of the prepared rotational level as a function of time, i.e., $n_{A'}(t)$ and $n_{A''}(t)$ by varying the time delay between IR and probe laser from 1 to 500 ns To determine the rate constants k_Λ, $k_R(A')$, and $k_R(A'')$ as defined in the Introduction, it was assumed that the concentrations $n_{A'}(t)$ and $n_{A''}(t)$ obey

$$\frac{dn_{A'}(t)}{dt} = -[k_\Lambda + k_R(A')]\cdot[H_2]\cdot n_{A'}(t) + k_\Lambda\cdot[H_2]\cdot n_{A''}(t), \tag{11}$$

$$\frac{dn_{A''}(t)}{dt} = -[k_\Lambda + k_R(A'')]\cdot[H_2]\cdot n_{A''}(t) + k_\Lambda\cdot[H_2]\cdot n_{A'}(t). \tag{12}$$

The two rate constants for the transitions between the Λ-doublet substates of the prepared rotational level are assumed to be equal and are denoted by k_Λ. This is reasonable, since the energy splitting in the Λ-doublets is lower than 0.75 cm^{-1} and, thus, detailed balance requires that the values of these rate constants agree within 0.4%. As already mentioned, $k_R(A')$ and $k_R(A'')$ are the total rate constants for all transitions out of the $\Pi(A')$ and the $\Pi(A'')$ Λ-doublet sublevel of the prepared rotational state. [H_2] denotes the density of H_2 molecules. Test measurements showed that within the time, where the concentrations $n_{A'}(t)$ and $n_{A''}(t)$ were probed, the density of OH molecules in nonprepared rotational levels is small compared to the population of the prepared one. Hence in Eqs. (11) and (12) secondary transitions back into the prepared rotational state can be neglected. Equations (11) and (12) can be solved analytically. The rate constants k_Λ, $k_R(A')$, and $k_R(A'')$ are fitted by plotting the solutions of Eqs. (11) and (12) with different values of k_Λ, $k_R(A')$, and $k_R(A'')$ together with the measured $n_{A'}(t)$ and $n_{A''}(t)$ and testing the agreement of calculation and experiment by a visual inspection of the plots.

For $Q_1(1)$ the neighbored satellite line $Q_1,(1)$ is excited together with the main line, since it is closer than the bandwidth of the probe laser, i.e., 0.21 cm^{-1}. In case of saturation the simultaneous excitation of two lines would lead to an excitation rate of 66%. Here the error is definitely smaller, because $Q_1,(1)$ is not saturated and not excited with the full laser power. Also the values of the rate constants are determined as mean values of the results obtained with $\Pi(A')$ prepared and $\Pi(A'')$ prepared, which leads to a further reduction of the error.

At a pressure of 250 mTorr quenching of the $^2\Sigma$ state by H_2 causes a considerable effect on the experimental results. Since different rotational levels are quenched with different efficiency,[42] the ratio of the values of $n(t)$ is measured incorrectly. However this error is small, because only the relative values of $n_{A'}(t)$, $n_{A''}(t)$ for a specific j enter into the fitting procedure and the rotational levels excited via the Q or R line, respectively, differ by only one quantum.

III. RESULTS

A. Crossed beam experiment

The experimental results for the system OH–H_2 are given in Figs. 5 and 6. The data are mean values of a number of measurements and the error bars are for one standard deviation of these mean values. Figure 5 shows the total excitation cross section averaged not only over initial, but also over final Λ-doublet states, i.e.,

$$\bar{\sigma}(j=1.5,\bar{\Omega}=1.5\rightarrow j',\bar{\Omega}') = 0.5\sum_{\epsilon,\epsilon'}\sigma(j=1.5,\bar{\Omega}=1.5,\epsilon\rightarrow j',\bar{\Omega}',\epsilon') = 0.5\cdot[\sigma_{A'}(J',\Omega')+\sigma_{A''}(J',\Omega')], \quad (13)$$

for various final rotational states in $^2\Pi_{3/2}$ and $^2\Pi_{1/2}$ as a function of excitation energy. The data are in arbitrary units, because the experimental results yield only relative cross sections. The $\sigma_{A''}$ are calculated via Eq. (10). No cross section is presented for the transition to $j'=1.5$, $\bar{\Omega}'=0.5$, because here the $\Pi(A'')$ Λ-doublet substate could not be probed separately due to line overlaps. The collision energy of 83 meV is indicated by the arrow. The idea behind this plot is to obtain a picture about the rotational energy transfer alone, i.e., to separate the effects of the selective population of Λ-doublets from rotational energy transfer. As can be seen, at $j'=5.5$, $\bar{\Omega}'=1.5$, and at $j'=4.5$, $\bar{\Omega}'=0.5$, almost all of the collision energy is converted to the rotational degree of freedom. For both $\bar{\Omega}'=1.5$ and $\bar{\Omega}'=0.5$ the cross sections decrease with increasing excitation energy, as expected from a power or energy gap law.

Because the spectral lines for the two spin manifolds are in the same range of wavelengths, the relative magnitudes of the cross sections for multiplet conserving ($\bar{\Omega}'=1.5$) and multiplet changing ($\bar{\Omega}'=0.5$) transitions could be accurately determined. Figure 5 shows that the cross sections for $\bar{\Omega}'=1.5$ and $\bar{\Omega}'=0.5$ are of the same order of magnitude. The cross sections for multiplet conserving transitions are generally larger and decrease more rapidly with increasing j' than the cross sections for multiplet changing transitions.

Figure 6 shows the ratio of the cross sections $\sigma_{A'}(j',\bar{\Omega}')/\sigma_{A''}(j',\bar{\Omega}')$ for $\bar{\Omega}'=1.5$ and $\bar{\Omega}'=0.5$ as a function of final rotational state. The $\sigma_{A'}/\sigma_{A''}$ are evaluated from the measured LIF signals using Eq. (9). They are $\geqslant 1$ for each $j',\bar{\Omega}'$ and increase with j' in both spin manifolds. At the lowest j' value a ratio of 1 or almost 1 is found for $\bar{\Omega}'=1.5$ or $\bar{\Omega}'=0.5$, respectively. Quantitatively the increase is steeper in $^2\Pi_{3/2}$. Within the probed j' levels a maximum of nearly 4 is reached, i.e., production of the $\Pi(A')$ substate is strongly favored. In fact, because $\Pi(A')$ is the lower Λ-doublet sublevel in the $^2\Pi_{3/2}$ state and the upper sublevel in the probed rotational states of $^2\Pi_{1/2}$,[10,32] this

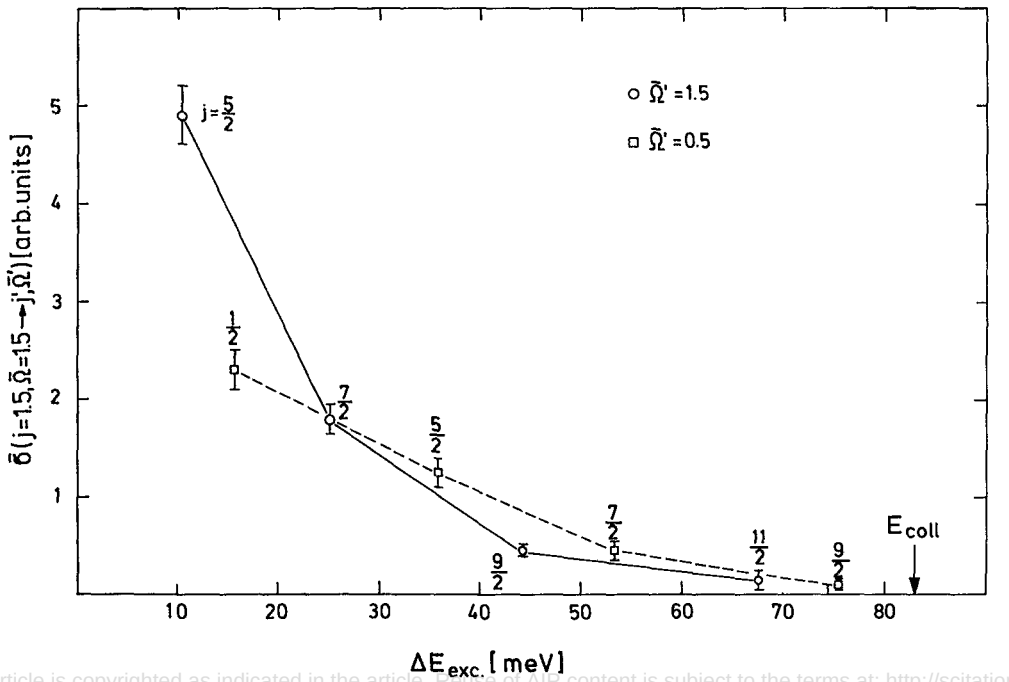

FIG. 5. Experimental OH–H_2 cross sections summed and averaged over the Λ-doublet substates for multiplet conserving (○) and multiplet changing transitions (□).

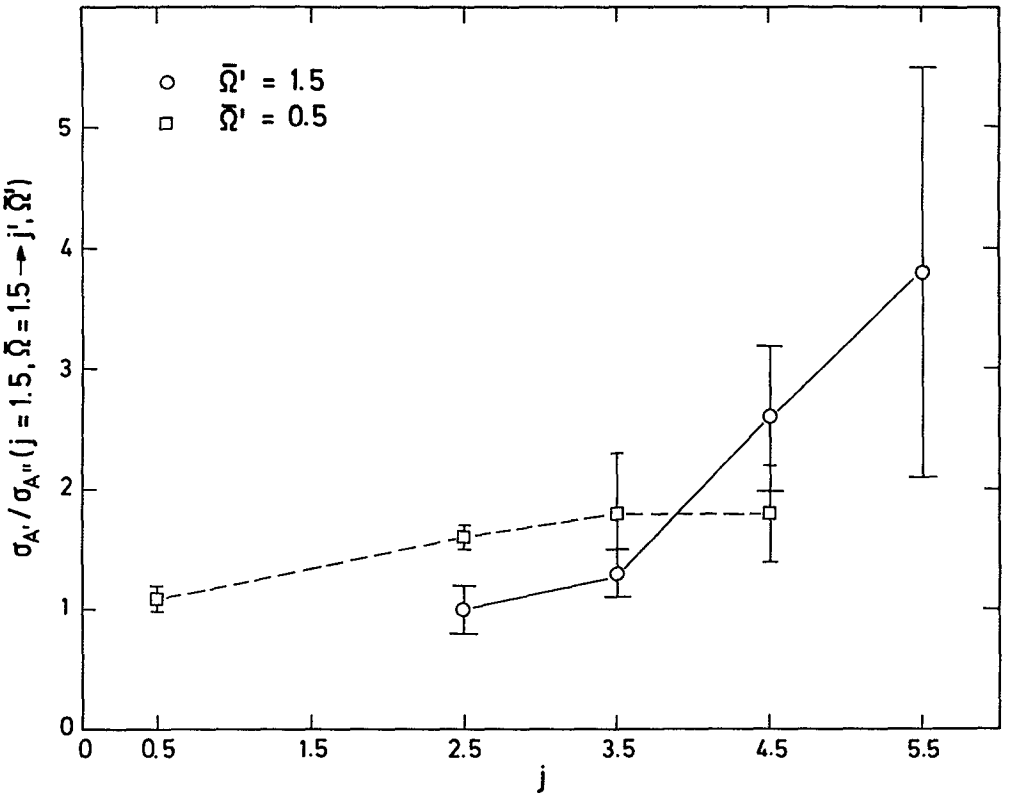

FIG. 6. Ratio of experimental OH–H_2 cross sections $\sigma_{A'}$ and $\sigma_{A''}$ as a function of final j; multiplet conserving transitions (○); multiplet changing transitions (□).

behavior corresponds to an anti-inversion in $^2\Pi_{3/2}$ and an inversion in $^2\Pi_{1/2}$. The implication of this result for astronomical OH masers have been already discussed.[43]

Table I summarizes the experimental results for OH–H_2 and OH–D_2 collisions. As in Figs. 5 and 6 the data represent mean values of a number of measurements and the errors are for one standard deviation of these values. For a single measurement the fluorescence signals are obtained by visually averaging the signals on the chart recorder paper and the $\sigma_{A'}$ and $\sigma_{A''}$ are determined as described in Sec. II A 3. Listed are the cross sections $\sigma_{A'}$ and $\sigma_{A''}$ for different j' and $\bar{\Omega}' = 0.5, 1.5$. The normalization of the OH–H_2 cross sections is the same as in Fig. 5. The results for OH–D_2 are normalized to the OH–H_2 cross sections at $j' = 2.5$, $\bar{\Omega}' = 1.5$. The cross sections $\sigma_{A'}$ and $\sigma_{A''}$ for $j' = 4.5$, $\bar{\Omega}' = 0.5$ and $\sigma_{A''}$ for $j' = 3.5$, $\bar{\Omega}' = 1.5$ were not measured for OH–D_2, because the ratio of signal to noise was too small.

Because the collision energy is nearly equal for OH–H_2 and OH–D_2, a direct comparison of the results is possible. Table I shows that similar values are obtained for the OH–H_2 and the OH–D_2 cross sections. In fact most of them agree within the range of experimental error. This indicates that there are no significant isotopic effects. In particular the

TABLE I. Experimental cross sections $\sigma_{A'}$ (first entry) and $\sigma_{A''}$ (second entry) for OH–H_2 and OH–D_2 in arbitrary units; OH–D_2 and OH–H_2 cross sections are normalized at $j' = 2.5$, $\bar{\Omega}' = 1.5$.

j'	OH–H_2	OH–D_2	OH–H_2	OH–D_2
	$\bar{\Omega}' = 1.5$		$\bar{\Omega}' = 0.5$	
0.5			1.2 ± 0.11 1.1 ± 0.14	0.89 ± 0.04 0.85 ± 0.11
1.5			1.09 ± 0.05	1.0 ± 0.12
2.5	2.45 ± 0.16 2.45 ± 0.52	2.45 ± 0.12 1.96 ± 0.30	0.76 ± 0.11 0.48 ± 0.07	0.56 ± 0.06 0.47 ± 0.11
3.5	1.01 ± 0.03 0.78 ± 0.12	1.34 ± 0.33	0.30 ± 0.08 0.17 ± 0.06	0.21 ± 0.06 0.13 ± 0.04
4.5	0.33 ± 0.03 0.13 ± 0.03	0.45 ± 0.19 0.23 ± 0.12	0.09 ± 0.03 0.05 ± 0.02	
5.5	0.11 ± 0.08 0.03 ± 0.02	0.08 ± 0.03 0.02 ± 0.018		

different population in the lowest rotational states of H_2 and D_2 has no remarkable influence on the collisional excitation of OH.

B. Double resonance experiment

It should be emphasized that the results of this difficult double resonance experiments could not be done in the completely collision-free regime. The results may be affected to a minor extent by collisions between OH and residual undissociated H_2O_2 in the flow system. Figure 7 shows typical time profiles for the concentration in the prepared Λ-doublet together with the concentration in the corresponding other Λ-doublet to the same initial prepared rotational state in $v = 1$. The curves represent calculated densities.

Figure 7 shows that the population in the nonprepared Λ-doublet first increases. At 150 ns the fraction of OH in this level is ~40% of the population in the prepared Λ-doublet substate. The population decreases later on, due to secondary collisions. This immediate sharp rise and delayed, gradual decrease indicates that the energy transfer between the Λ-doublet sublevels of a given j state is much faster than rotational or multiplet transitions.

The first column of Table II shows the fitted rate constants k_Λ, $k_R(A')$, and $k_R(A'')$. Also listed are rate constants for OH–H_2O_2 collisions, obtained from experiments with pure H_2O_2. For $j = 4.5$ only the decay in the population of the prepared level could be probed. Here the fraction of OH in $v = 1$ is very small and S/N became too bad. Hence for $j = 4.5$ it was hardly possible to derive rate constants. The k_Λ, $k_R(A')$, and $k_R(A'')$ could be varied over a wide range of values without a significant variation in the calculated decay of the prepared level. In Table II for the rate constants for $j = 4.5$ the range of values is given, where a visual comparison of calculated and measured $n(t)$ showed a good agreement. For j initial = 1.5 the concentrations in both Λ-doublet sublevels could be probed as function of time and hence the rate constants could be determined more precisely. However due to the remaining uncertainties in the experimental data it was not possible to decide which values of k_Λ, $k_R(A')$, and $k_R(A'')$ fit the experimental data best. The values given in Table II are mean values for a number of determinations of k_Λ, $k_R(A')$, and $k_R(A'')$, which yielded a good agreement between calculation and experiment. The error limits are for one standard deviation of these values.

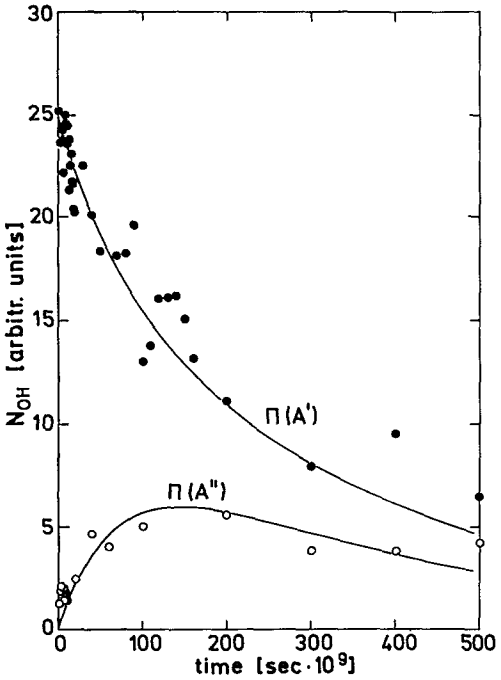

FIG. 7. Populations in the prepared (●) and the nonprepared (○) Λ-doublet substate of OH($^2\Pi_{3/2}$, $j = 1.5$, $v = 1$) as functions of time; the curves show calculated populations.

TABLE II. OH–H_2 rate constants k_Λ, $k_R(A')$, and $k_R(A'')$ in $cm^3/s \times 10^{10}$, $T = 300$ K.

Collision system	Initial j	Initial $\bar{\Omega}$		This work (expt.) $v = 1$	DFA (calc.) $v = 0$
OH–H_2	1.5	1.5	k_Λ	5.1 ± 1.1	1.43
			$k_R(A')$	2.8 ± 2.0	1.41
			$k_R(A'')$	4.4 ± 1.9	1.59
OH–H_2	4.5	1.5	k_Λ	0.1–5	0.32
			$k_R(A')$	1.5–6.5	2.50
			$k_R(A'')$	1.5–6.5	2.29
OH–H_2O_2	4.5	1.5	k_Λ	1–10	
			$k_R(A')$	5–9	
			$k_R(A'')$	5–9	

The rate constants for OH–H_2O_2 collisions were measured to estimate errors introduced by collisions of OH with H_2O_2 instead of H_2. Table II shows that the values of k_Λ, $k_R(A')$, and $k_R(A'')$ are larger for OH–H_2O_2 than for OH–H_2, i.e., hydrogen peroxide transfers energy more efficiently than hydrogen. However, for the relative concentrations of H_2 and H_2O_2 used in the experiment, it can be estimated that the effects of OH–H_2O_2 interactions are small compared with the other error limits for the OH–H_2 rate constants in Table II.

IV. THEORETICAL

The preference in the population of the $\Pi(A')$ Λ-doublet substate found in the crossed beam experiment could be reproduced only qualitatively in an earlier calculation.[19] It was shown therein that the populations of the Λ-doublet substates are strongly influenced by the shape of the difference potential $V_{A'} - V_{A''}$. In this study scattering calculations with different $V_{A'} - V_{A''}$ are performed to study in some more detail than in Ref. 19 the effect of the difference potential on the "Λ-doublet substate ratios" $\sigma_{A'}/\sigma_{A''}$ and the Λ-doublet substate averaged cross sections $\bar{\sigma}$.

The theoretical framework for collisions of a $^2\Pi$ molecule with a structureless particle is described in detail elsewhere.[18,19,44] Here only some important features of the potential matrix will be discussed.

For $^2\Pi$ molecules falling within Hund's coupling case (a) multiplet conserving transitions ($\bar{\Omega} = \bar{\Omega}'$) are promoted solely by the sum potential $V_{A'} + V_{A''}$, whereas transitions

with $\bar{\Omega} \neq \bar{\Omega}'$ are related exclusively to the difference potential $V_{A'} - V_{A''}$. Also the values of the cross sections for ϵ-conserving or ϵ-changing transitions do not depend on the sign of the initial ϵ implying that a preferential population of one Λ-doublet substate cannot occur.

The OH radical cannot be classified by Hund's coupling cases: at low j it is close to Hund's case (a) whereas at high j it is closer to Hund's case (b).[19,45] Here $\bar{\Omega}$-conserving or $\bar{\Omega}$-changing transitions are no longer promoted exclusively by the sum or difference potential, respectively. In addition for $\epsilon = \epsilon'$ as well as for $\epsilon \neq \epsilon'$ now the cross sections may have different values and thus a preferential population of one Λ-doublet substate can occur. This propensity toward population of a particular Λ-doublet substate is opposite for molecules of π^1 and π^3 electron occupancy:[23] For the latter $V_{A''}$ is more repulsive than $V_{A'}$ whereas for molecules of π^3 electron occupancy $V_{A''}$ is more repulsive.

The program used for the calculations is the same as in Ref. 19. It is based on the treatment of collisions with Π molecules by Alexander.[18] Three expansion coefficients of the sum potential ($V_{\lambda 0}, \lambda = 0,1,2$) and one expansion coefficient of the difference potential ($V_{\lambda 2}, \lambda = 2$) are included. The coefficients of the sum potential are adopted from the *ab initio* surfaces of Kochanski and Flower[46] KF potential). In order to simplify the problem only collisions of OH with para-H_2 ($j = 0$) are calculated. This is reasonable, since the crossed beam data for H_2 and D_2 show no significant differences indicating that initial rotation of H_2 is unimportant. The calculations are performed at the collision energy of the crossed beam experiment, i.e., 83 meV. Because of the large number of energetically open states at this energy the coupled states (CS) approximation[44] is used to reduce the number of coupled equations. Previous work[5(a),19,22] has shown that this approximation yields satisfactory results at 83 meV collision energy.

The calculations showed that an equal population of the Λ-doublet substates, i.e., $\sigma_{A'} = \sigma_{A''}$, is obtained with $V_{22} = 0$ and changing the sign of V_{22} exactly reverses the ratio $\sigma_{A'}/\sigma_{A''}$ for all $j', \bar{\Omega}'$. This is not surprising, since changing the sign of V_{22} is equivalent to exchanging $V_{A'}$ and $V_{A''}$. It is agreement with the above predictions and indicates that the value of $\sigma_{A'}/\sigma_{A''}$ reflects the magnitude of the difference potential. On the other hand it could not be proved that a larger difference potential in every case increases the preferential population of one Λ-doublet substate. Often for some final quantum states increased values for $\sigma_{A'}/\sigma_{A''}$ as well as decreased values for the other $j', \bar{\Omega}'$ were found. In general, the $\sigma_{A'}/\sigma_{A''}$ for $\bar{\Omega}' = 1.5$ are more sensitive on V_{22} than the $\sigma_{A'}/\sigma_{A''}$ for $\bar{\Omega}' = 0.5$. Only towards higher j' ($j' = 3.5,4.5$) the effect of V_{22} on the latter is comparable to $^2\Pi_{3/2}$, whereas it is less pronounced for $j' = 0.5,1.5,2.5$. For the $\sigma_{A'}/\sigma_{A''}$ with $\bar{\Omega}' = 0.5$ a trend to opposite effects of V_{22} for $j' = 0.5$ and $j' = 3.5,4.5$ is found: increasing V_{22} leads to decreased values of the $\sigma_{A'}/\sigma_{A''}$ for $j' = 0.5$ and increased values for $j' = 3.5,4.5$ or vice versa. The sensitivity of the Λ-doublet substate averaged cross sections on V_{22} is greater for $\bar{\Omega}' = 0.5$ than for $\bar{\Omega}' = 1.5$. This is not surprising, since OH is close to Hund's case (a) for the j' considered here. The effect on the $\bar{\sigma}$ for $\bar{\Omega}' = 1.5$ is greater towards higher j' reflecting the increasing deviation from Hund's case (a).

V. DISCUSSION AND CONCLUSIONS

A. Difference potential and integral cross sections

Figure 5 shows that the preferential population of the $\Pi(A')$ Λ-doublet substate increases with final j for both $\bar{\Omega}' = 0.5$ and $\bar{\Omega}' = 1.5$. As indicated, a preferential population of one Λ-doublet substate can occur only, if the $^2\Pi$ molecule does not fall within Hund's coupling case (a). Thus, Fig. 5 reflects that there is a deviation from Hund's case (a) with OH, which increases with j. On the contrary, the NO molecule can be well described within Hund's case (a) even at high rotational states.[31] Accordingly, no preferential population of one Λ-doublet sublevel was found in collisions of NO with rare gases.[31,47]

For NO–Ar the Λ-doublet averaged cross sections $\bar{\sigma}(j = 0.5, \bar{\Omega} = 0.5 \rightarrow j', \bar{\Omega}' = 0.5)$ show an interesting behavior. The decay of their values towards higher j' is superimposed by an oscillatory structure, i.e., for low j' transitions with $\Delta j = 2$ are preferred.[31,47] It could be shown that this effect is related to a dominant V_{20} coefficient of the NO–Ar sum potential. For OH–H_2 the expansion coefficients V_{10} and V_{20} have comparable values.[5(a)] Accordingly, a monotonic decay of the cross sections with $\Delta\bar{\Omega} = 0$ is obtained. The physical reason for this difference is the almost homonuclear character of NO on one hand, and the heteronuclear character of OH on the other hand.

The more recent theoretical studies of the OH–H_2 system[19–21] obtain—in agreement with the crossed beam experiment—a population inversion in the Λ-doublets of $^2\Pi_{1/2}$ and an anti-inversion in $^2\Pi_{3/2}$. Earlier errors,[16,17] which led to an opposite Λ-doublet substate preference, are avoided therein. In the calculations of Refs. 19 and 20 the same sum potential is used, i.e., three expansion coefficients of the KF potential. However, a different difference potential is employed: Schinke and Andresen (SA)[19] use the V_{22} coefficient of the KF potential [V_{22}(KF)], whereas Dewangan, Flower, and Danby (DFD)[20] use the V_{22} coefficient of the KF potential reduced by a factor $\frac{1}{2}$ [V_{22}(KF)/2]. [The actual potential used in Ref. 20 is V_{22}(KF). However, an error of a factor of 2 was made in the scattering matrix,[21] which is equivalent to using V_{22}(KF)/2.]

In Fig. 8 Λ-doublet substate averaged cross sections $\bar{\sigma}(j = 1.5, \bar{\Omega} = 1.5 \rightarrow j', \bar{\Omega}' = 0.5,1.5)$ calculated in Refs. 19 and 20 are compared to the crossed beam data. Calculated and measured values are normalized at $j' = 2.5, \bar{\Omega}' = 1.5$. Because no cross sections for 83 meV are published by DFD, they were estimated by averaging the cross sections for 69 and 103 meV in Table I of Ref. 20.

For $\bar{\Omega}' = 1.5$ both calculations lead to a good agreement with the experiment. This is not surprising, since they are performed with the same sum potential. Also the values of the experimental cross sections for $\bar{\Omega}$-changing transitions relative to each other are well reproduced with V_{22}(KF) and V_{22}(KF)/2: measured and calculated cross sections show almost the same dependence of j'.

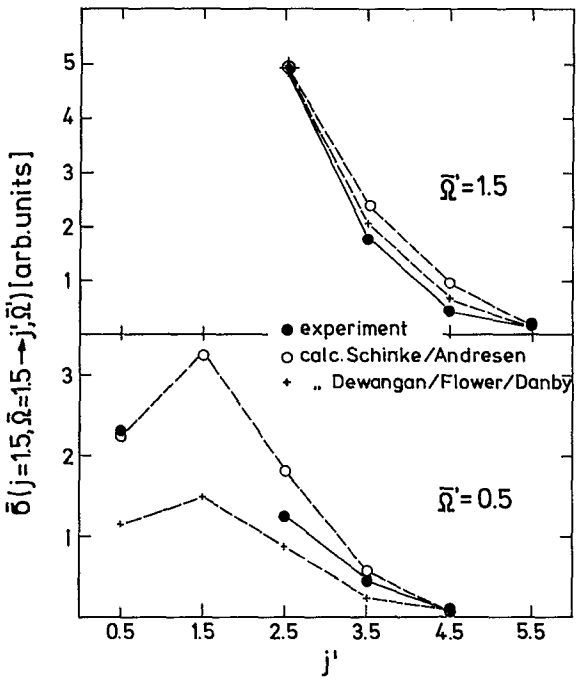

FIG. 8. Comparison between calculated and experimental Λ-doublet substate averaged cross sections for OH–H_2; $E_{coll} = 83$ meV; the calculated cross sections are adopted from Schinke and Andresen (Ref. 19) and Dewangan, Flower, and Danby (Ref. 20); all cross sections are normalized at $j' = 2.5$, $\bar{\Omega}' = 1.5$.

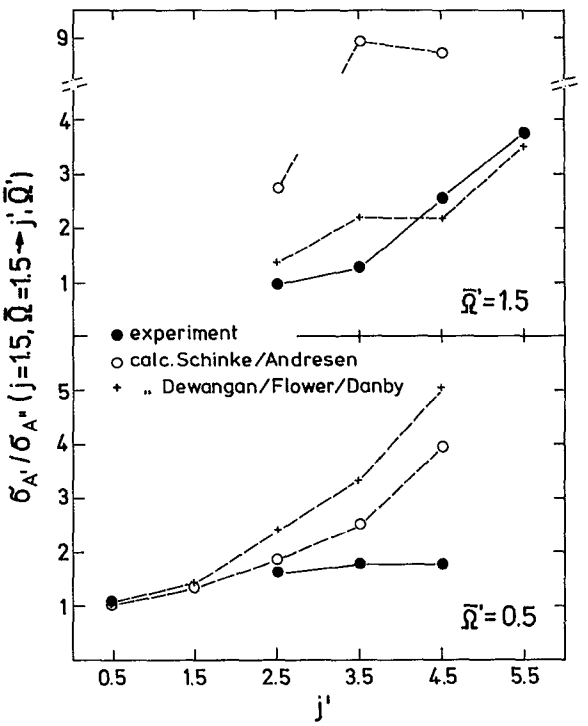

FIG. 9. Comparison between calculated and experimental ratios $\sigma_{A'}/\sigma_{A''}$ for OH–H_2; the calculated ratios are adopted from Schinke and Andersen (Ref. 19) and Dewangan, Flower, and Danby (Ref. 20).

It is interesting that both calculations yield an increase in the cross section for $\bar{\Omega}' = 0.5$ between $j' = 0.5$ and $j' = 1.5$, although the overall trend is a decrease with increasing j'. No experimental value for $j' = 1.5$, $\bar{\Omega}' = 0.5$ is displayed, because the cross section $\sigma_{A''}$ could not be measured.

The ratio of the cross sections for $\bar{\Omega}' = 1.5$ to the cross sections for $\bar{\Omega}' = 0.5$ is overestimated with V_{22}(KF)/2. Here only the results of SA are in good agreement with the experiment. This indicates that compared to the sum potential V_{22}(KF) has an almost correct magnitude, whereas V_{22}(KF)/2 is too small.

A comparison of Fig. 8 to cross sections obtained in collisions of NO with Ar[31,47] shows that the ratio of the cross sections with $\Delta\bar{\Omega} = 0$ vs the cross sections with $\Delta\bar{\Omega} \neq 0$ is greater for NO–Ar than for OH–H_2. Here is reflected that in the coupling potential of NO–Ar the ratio of the magnitudes of the sum vs the difference potential[48] is larger than with the coupling potentials for OH–H_2 discussed here.

Experimental and calculated ratios of the populations in the Λ-doublet substates $\sigma_{A'}/\sigma_{A''}$ are compared in Fig. 9. The cross sections of DFD for 83 meV are estimated in the same manner as in Fig. 8. Experiment and calculations show a preferential population of the $\Pi(A')$ Λ-doublet substate. This propensity can be related to the π^3 electron occupancy of OH.[23] In collisions of $CH(X\,^2\Pi)$, which has a single electron in the π orbital, a reversed propensity has been found.[49]

With V_{22}(KF) the experimental values are well reproduced only for the lower final rotational states in $^2\Pi_{1/2}$, whereas particularly in $^2\Pi_{3/2}$ they are strongly overestimated. The results of DFD are in better agreement with the experiment, although for $\bar{\Omega}' = 0.5$ the experimental values are more overestimated than with V_{22}(KF). As in our calculations here is found that a lower difference potential may lead to an increase in the overpopulation of a Λ-doublet substate for some j',$\bar{\Omega}'$ and not to an overall decrease.

A good agreement between theory and experiment for the Λ-doublet substrate averaged cross sections *and* the ratios $\sigma_{A'}/\sigma_{A''}$ may be achieved by using a smaller sum potential. With V_{22}(KF)/2 only the ratio of the cross sections with $\Delta\bar{\Omega} = 0$ vs the cross sections with $\Delta\bar{\Omega} \neq 0$ is in bad agreement with the experiment. Thus, the overall agreement with the experiment could be improved by using a smaller sum potential together with a difference potential comparable (or equal) to V_{22}(KF)/2. Note that no absolute values for the cross sections are measured and, thus, the cross sections for transitions within $^2\Pi_{3/2}$, which essentially are affected by a variation of the sum potential, may have lower values than given in Table I.

B. OH–H_2 rate constants

Recently OH–H_2 rate constants were published by Dewangan, Flower, and Alexander (DFA).[21] In Table II their data are compared to the results of the double resonance experiment. Since no rate constants for 300 K are published by DFA, they were estimated by a linear interpolation of the values for 240 and 480 K in Table II of Ref. 21. The theoretical values for $k_R(A')$ and $k_R(A'')$ are obtained by a summation over the product states. Note that experimental and calculated rate constants are for different vibrational levels, i.e., $v = 1$ and $v = 0$, respectively. However, this dif-

ference should cause a minor effect, since in $v = 1$ the OH bond length changes by only 10%. This has been documented for He–Na_2.[50]

Experiment and calculations yield comparable values for the k_Λ, $k_R(A')$, and $k_R(A'')$. For j-init. $= 1.5$ the results of the calculations are 2–3 times smaller than the measured values and for j-init. $= 4.5$ they are within the range obtained in the experiment. In both the experiment and the calculations the energy transfer between the Λ-doublet substates is found more efficient for $j = 1.5$ than for $j = 4.5$. For $j = 1.5$, k_Λ has about the same value than $k_R(A')$ or $k_R(A'')$, respectively, and for $j = 4.5$ the calculated value for k_Λ is only about six times smaller than the values for k_R. This shows the high efficiency of the energy transfer between the Λ-doublet substates compared to the energy transfer between rotational states. Note that the k_R represent the sum of all rate coefficients for transitions from the prepared into other rotational (and vibrational) states. The experimental results in Table II have to be considered with some care, because the signal to noise ratio was not great.

To obtain more information about the dynamics of OH–H_2 collisions, further experiments about Λ-doublet resolved rate coefficients (or cross sections) at different temperatures (or energies) would be of great help. A way pursued right now is the preparation of a single Λ-doublet substate by "pump and dump" techniques, which hopefully yields better signal to noise than direct infrared excitation.

ACKNOWLEDGMENT

We thank Dr. R. Schinke for the coupled states program and for many helpful discussions.

[1] M. J. Reid and J. M. Moran, Annu. Rev. Astron. Astrophys. **19**, 231 (1981); M. Elitzur, Rev. Mod. Phys. **54**, 1225 (1982).
[2] W. D. Gwinn, B. E. Turner, W. M. Goss, and G. L. Blackman, Astrophys. J. **179**, 789 (1973); M. Bertojo, A. C. Cheung, and C. H. Townes, *ibid.* **208**, 914 (1976).
[3] R. N. Dixon and D. Field, Proc. R. Soc. London Ser. A **368**, 99 (1979).
[4] M. Shapiro and H. Kaplan, J. Chem. Phys. **71**, 2182 (1979).
[5] (a) D. P. Dewangan and D. R. Flower, J. Phys. B **14**, 2179 (1981); (b) D. P. Dewangan and D. R. Flower, *ibid.* **16**, 2157 (1983).
[6] R. P. Mariella, B. Lantzsch, V. T. Maxson, and A. C. Luntz, J. Chem. Phys. **69**, 5411 (1978); A. C. Luntz, *ibid.* **73**, 1143 (1980); K. Kleinermanns and J. Wolfrum, *ibid.* **80**, 1446 (1984); K. Kleinermanns and J. Wolfrum, Chem. Phys. Lett. **104**, 157 (1984).
[7] (a) P. Andresen, G. S. Ondrey, B. Titze, and E. W. Rothe, J. Chem. Phys. **80**, 2548 (1984); (b) P. Andresen and E. W. Rothe, J. Chem. Phys. **82**, 3634 (1985).
[8] G. Ondrey, N. van Veen, and R. Bersohn, J. Chem. Phys. **78**, 3732 (1983).
[9] A. Jacobs, K. Kleinermanns, H. Kuge, and J. Wolfrum, J. Chem. Phys. **79**, 3162 (1983).
[10] M. H. Alexander and P. J. Dagdigian, J. Chem. Phys. **80**, 4325 (1984).
[11] M. H. Alexander, P. Andresen, R. Bacis, R. Bersohn, F. J. Comes, P. J. Dagdigian, R. N. Dixon, R. W. Field, G. W. Flynn, K. H. Gericke, E. R. Grant, B. J. Howard, J. R. Huber, D. S. King, J. L. Kinsey, K. Kleinermanns, K. Kuchitsu, A. C. Luntz, A. J. McCaffery, B. Pouilly, H. Reisler, S. Rosenwaks, E. W. Rothe, M. Shapiro, J. P. Simons, R. Vasudev, J. R. Wiesenfeld, C. Wittig, and R. N. Zare, J. Chem. Phys. **89**, 1749 (1988).
[12] P. Andresen, D. Häusler, and H. W. Lülf, J. Chem. Phys. **81**, 571 (1984).
[13] J. Dufayard and O. Nedelec, Chem. Phys. **71**, 279 (1982); O. Nedelec and J. Dufayard, *ibid.* **84**, 167 (1984); O. Nedelec and J. Dufayard, Chem. Phys. Lett. **105**, 371 (1986); C. Dufour, B. Pinchemel, M. Douay, J. Schamps, and M. H. Alexander, Chem. Phys. **98**, 315 (1985).
[14] (a) R. A. Copeland and D. R. Crosley, J. Chem. Phys. **81**, 6400 (1984); (b) Aa. S. Sudbo and M. M. T. Loy, *ibid.* **76**, 3646 (1982); (c) Y. Honguh, F. Matsushima, R. Katayama, and T. Shimizu, *ibid.* **83**, 5052 (1985); (d) F. Menard-Bourcin, T. Delaporte, and J. Menard, *ibid.* **84**, 201 (1986).
[15] S. Green and R. N. Zare, Chem. Phys. **7**, 62 (1975).
[16] R. N. Dixon, D. Field, and R. N. Zare, Chem. Phys. Lett. **122**, 310 (1985).
[17] D. P. Dewangan and D. R. Flower, J. Phys. B **18**, L137 (1985).
[18] M. H. Alexander, Chem. Phys. **92**, 337 (1985).
[19] R. Schinke and P. Andresen, J. Chem. Phys. **81**, 5644 (1984).
[20] D. P. Dewangan, D. R. Flower, and G. Danby, J. Phys. B **19**, L747 (1986).
[21] D. P. Dewangan, D. R. Flower, and M. H. Alexander, Mon. Not. R. Astron. Soc. **226**, 505 (1987).
[22] G. C. Corey and M. H. Alexander, J. Chem. Phys. **88**, 6931 (1988).
[23] P. J. Dagdigian, M. H. Alexander, and K. Liu, J. Chem. Phys. **91**, 839 (1989).
[24] D. E. Powers, J. B. Hopkins, and R. E. Smalley, J. Chem. Phys. **85**, 2711 (1981).
[25] D. L. Monts, T. G. Dietz, M. A. Duncan, and R. E. Smalley, Chem. Phys. **45**, 133 (1980); M. Heaven, T. A. Miller, and V. E. Bondybey, Chem. Phys. Lett. **84**, 1 (1981).
[26] H. Johnston and R. Graham, J. Phys. Chem. **77**, 62 (1973); F. Biaume, J. Photochem. **2**, 139 (1973/74).
[27] H. W. Lülf and P. Andresen, in *Rarefied Gas Dynamics*, edited by O. M. Belotserkovskii, M. N. Kogan, S. S. Kutateladze, and A. K. Rebrov (Plenum, New York, 1985), Vol. 2.
[28] J. B. Anderson and J. B. Fenn, Phys. Fluids **8**, 780 (1965).
[29] A. H. Shapiro, *The Dynamics and Thermodynamics of Compressible Fluid Flow* (Ronald, New York, 1953), Vol. 1; H. R. Murphy and D. R. Miller, J. Phys. Chem. **88**, 4474 (1984).
[30] R. E. Smalley, D. H. Levy, and L. Wharton, J. Chem. Phys. **64**, 3266 (1976); H. Zacharias, M. M. T. Loy, P. A. Roland, and A. Sudbo, *ibid.* **81**, 3148 (1984).
[31] H. Joswig, P. Andresen, and R. Schinke, J. Chem. Phys. **85**, 1904 (1986).
[32] (a) G. H. Dieke and H. M. Crosswhite, J. Quant. Spectrosc. Radiat. Transfer **2**, 97 (1962); (b) E. A. Moore and W. G. Richards, Phys. Scr. **3**, 223 (1971); (c) J. A. Coxon, Can. J. Phys. **58**, 933 (1980).
[33] U. Hefter and K. Bergmann, in *Atomic and Molecular Beam Methods*, edited by G. Scoles (Oxford University, New York, 1988), Vol. 1.
[34] P. J. Dagdigian, in *Atomic and Molecular Beam Methods*, edited by G. Scoles (Oxford University, New York, 1988), Vol. 1.
[35] D. Häusler, P. Andresen, and R. Schinke, J. Chem. Phys. **87**, 3949 (1987).
[36] D. J. Brink, D. Proch, D. Basting, K. Hohla, and P. Lokai, Laser Optoelek. **3**, 41 (1982).
[37] *Tables of Wavenumbers for the Calibration of Infrared Spectrometers*, 2nd ed., compiled by A. R. H. Cole (Pergamon, Oxford, 1977); J. M. Flaud, C. Camy-Peyret, and R. A. Toth, *Water Vapour Line Parameters from Microwave to Medium Infrared* (Pergamon, Oxford, 1981).
[38] L. B. Kreuzer and C. K. N. Patel, Science **173**, 45 (1971).
[39] J. P. Maillard, J. Chauville, and A. W. Mantz, J. Mol. Spectrosc. **63**, 120 (1976); T. Amano, *ibid.* **103**, 436 (1984).
[40] C. L. Lin, N. K. Rohatgi, and W. B. DeMore, Geophys. Res. Lett. **5**, 113 (1978); M. Suto and L. C. Lee, Chem. Phys. Lett. **98**, 152 (1983).
[41] S. R. Langhoff, H. J. Werner, and P. Rosmus, J. Mol. Spectrosc. **118**, 507 (1986).
[42] R. A. Copeland, M. J. Dyer, and D. R. Crosley, J. Chem. Phys. **82**, 4022 (1985).
[43] P. Andresen, Astron. Astrophys. **154**, 42 (1986).
[44] M. H. Alexander, J. Chem. Phys. **76**, 5974 (1982).
[45] G. C. Dousmanis, T. M. Sanders, Jr., and C. H. Townes, Phys. Rev. **100**, 1735 (1955).
[46] E. Kochanski and D. R. Flower, Chem. Phys. **57**, 217 (1981).
[47] T. Orlikowski and M. H. Alexander, J. Chem. Phys. **79**, 6006 (1983).
[48] G. C. Nielson, S. A. Parker, and R. T. Pack, J. Chem. Phys. **66**, 1396 (1977).
[49] R. G. Macdonald and K. Liu, J. Chem. Phys. **91**, 821 (1989).
[50] W. Müller and R. Schinke, J. Chem. Phys. **75**, 1219 (1981).